Published in final edited form as:
Mol Oral Microbiol. 2013 April ; 28(2): . doi:10.1111/omi.12014.

Phenotypic characterization of the foldase homologue PrsA in *Streptococcus mutans*

Lihong Guo[1], **Tingxi Wu**[1,4], **Wei Hu**[1,5], **Xuesong He**[1], **Shivani Sharma**[2], **Paul Webster**[3], **James K Gimzewski**[2], **Xuedong Zhou**[4], **Renate Lux**[1], and **Wenyuan Shi**[1,*]

[1]School of Dentistry, University of California, Los Angeles, CA90095, U.S.A

[2]California Nano Systems Institute and Department of Chemistry and Biochemistry, University of California, Los Angeles, CA90095, U.S.A

[3]Ahmanson Advanced Electron Microscopy and Imaging Centre, House Research Institute, 2100 W 3rd St, Los Angeles, CA 90057, U.S.A

[4]West China School of Stomatology, Sichuan University, Chengdu 610041, China

[5]State Key Laboratory of Microbial Technology, College of Life Science, Shandong University, Jinan 250100, China

SUMMARY

Streptococcus mutans is generally considered to be the principal etiological agent for dental caries. Many of the proteins necessary for its colonization of the oral cavity and pathogenesis are exported to the cell surface or the extracellular matrix, a process that requires the assistance of the export machineries. Bioinformatic analysis revealed that the *S. mutans* genome contains a *prsA* gene, whose counterparts in other gram positive bacteria, including *Bacillus* and *Lactococcus* encode functions involved in protein post-export. In this study, we constructed a PrsA-deficient derivative of *S. mutans* and demonstrated that the *prsA* mutant displayed an altered cell wall/membrane protein profile as well as cell surface related phenotypes, including auto-aggregation, increased surface hydrophobicity, and abnormal biofilm formation. Further analysis revealed that the disruption of the *prsA* gene resulted in reduced insoluble glucan production by cell surface localized glucosyltransferases, and mutacin as well as cell surface-display of a heterologous expressed GFP fusion to the cell surface protein SpaP. Our study suggested that PrsA in *S. mutans* encodes functions similar to the ones identified in *Bacillus*, and thus is likely involved in protein post-export.

Keywords

foldase protein PrsA; protein secretion; *Streptococcus mutans*

INTRODUCTION

As the primary etiological agent of dental caries in humans (Hamada & Slade, 1980), *Streptococcus mutans* relies on the activities of secreted or cell surface localized proteins to interact with other oral bacteria, colonize the oral cavity and exert its pathogenesis. Previous studies have shown that *S. mutans* employs various mechanisms to deliver proteins across the cell membrane. The general secretory (Sec) translocation channel is the major secretion

*Corresponding author: Wenyuan Shi, School of Dentistry, University of California, 10833 Le Conte Avenue, Los Angeles, CA90095. Tel. 13108258356, Fax. 13107947194, wenyuan@ucla.edu.

apparatus in proteins translocation across the cytoplasmic membrane (Fekkes & Driessen, 1999; Muller *et al.*, 2001). In addition, *S. mutans* also contains certain specific secretion systems. For example, specific ATP-binding cassette transporters were found to be responsible for direct translocation of the bacteriocins across the cytoplasmic membrane (van Belkum *et al.*, 1997). Most proteins translocated across the cell membrane via above pathways are considered to be delivered in an unfolded conformation across the cytoplasmic membrane into the interface between cytoplasmic membrane and cell wall peptidoglycan (Matias & Beveridge, 2006; Matias & Beveridge, 2008; Sarvas *et al.*, 2004). Due to the high cation concentration, as well as the low pH and high density of negative charge within the cytoplasmic membrane- cell wall peptidoglycan interface (Sarvas *et al.*, 2004), protein chaperones as well as foldases are required to ensure the proper folding of these proteins after export. However, the components and their roles in the folding and stabilize proteins to their active form are poorly characterized in *S. mutans*.

The foldase protein PrsA is found ubiquitously in the genomes of all Gram-positive bacteria including *S. mutans*. In the Group A streptococcus including *S. pyogenes*, PrsA was found to be required for the final maturation steps of SpeB, a pluripotent cysteine protease and an important virulence factor (Ma *et al.*, 2006). The role of PrsA in assisting the folding and stability of exported proteins has been extensively studied in *Bacillus* and *Lactococcus.* In *B. subtilis*, the extracytoplasmically located PrsA has been shown to be critically important *in vivo* for the proper conformation of various exoproteins (Jacobs *et al.*, 1993), and considered as an essential rate-limiting component of the secretion machinery (Kontinen & Sarvas, 1993). It influences neither the expression nor the translocation of exoproteins but is required for their correct conformation and stability in the post-translocational phase of secretion (Hyyryläinen *et al.*, 2001; Vitikainen *et al.*, 2001). In *L. lactis*, the PrsA- like protein triggers the folding of the translocated lipase (Drouault *et al.*, 2002). Over-expression of *B. subtilis* PrsA also resulted in increased heterologous protein expression in *L. lactis*, presumably by allowing more efficient protein folding (Lindholm *et al.*, 2006).

In *S. mutans*, the predicted PrsA protein contains 333 amino acids with a molecular mass of ~36 kDa. It includes a predicted signal sequence at the N-terminus. However, no cellular function has been assigned to this protein. In this study, by constructing a *prsA*-deficient strain and performing an array of phenotypic analyses, we sought to investigate the biological functions of PrsA in *S. mutans*.

METHODS

Bacterial strains and growth conditions

E. coli strain DH5α was used for cloning as well as plasmid amplifications and grown in Luria-Bertani (LB) medium aerobically at 37 °C. *S. mutans* strain UA140 (wild type), UA140 *prsA*-deficient strain, as well as UA140 pHluorin-SpaP fusion strain and its corresponding *prsA*-deficient strain were cultured in Todd-Hewitt (TH) media (Difco) at 37° Cin the presence of 5% CO_2. For selection of antibiotic-resistant colonies after genetic transformation, spectinomycin (100 μg/mL for *E. coli* or 800 μg/mL for *S. mutans*) or kanamycin (150 μg/mL for *E. coli* or 800 μg/ml for *S. mutans*) was added to the medium.

Strain construction

The open reading frame for the predicted *prsA* gene (GenBank accession no. AAN58382) was annotated in the *S. mutans* UA159 genome database (http://www.genome.ou.edu/smutans.html). BLASTn and BLASTp sequence homology analyses were performed by using the BLAST network service of the National Center of Biotechnology Information (NCBI), Bethesda, MD. The pFW5 vector (Podbielski *et al.*, 1996) was employed for

generating a mutant derivative of *S. mutans* wild type strain UA140 (Qi *et al.*, 2001) carrying a deletion in the *prsA* gene. *S. mutans* UA140 genomic DNA served as a template to amplify the *prsA* upstream region with the primer pair upF (5′-CCGCTCGAGCGCAAACCACATCCACAGGG) which contains a *XhoI* site incorporated at its 5′ end and upR (5′-CCCAAGCTTCACAAGTCCTGTAGCAATCG) which has a *HindIII* site incorporated at its 5′ end, while the corresponding downstream region was obtained using downF (5′-ACATGCATGCCAGCAGCAAGCGGAAGTGGC) which carries a *SphI* site incorporated at its 5′ end and downR (5′-TCCCCCCGGGAGCATCATCACGGAAGTAAT) with a *XmaI* site incorporated at its 5′ end (the restriction enzyme recognition sites are underlined). The fragments were generated using *Pfu* polymerase (Stratagene) and subsequently inserted into the two multiple cloning sites of pFW5 vector respectively. The resulting recombinant plasmid pFW5-*prsA* was confirmed by restriction analysis, PCR amplification and DNA sequencing. Plasmid pFW5-*prsA* was then linearized using a unique *NheI* site in the vector backbone and transformed into *S. mutans* UA140 via competence-stimulating peptide (CSP)-induced natural transformation (Kreth *et al.*, 2005). CSP was a gift from C3 Jian Inc. (Los Angeles, CA). Transformants were selected on TH agar containing 800 μg/mL of spectinomycin. The resulting *prsA* deletion mutant was confirmed by PCR and sequencing.

The GFP coding sequence was in-frame inserted via overlapping PCR between the second and third amino acids after the identified signal-peptide cleavage site of SpaP (Kelly *et al.*, 1989), a surface protein antigen-encoding gene of *S. mutans*. The resulting fragment was then ligated downstream of the lactate dehydrogenase gene (*ldh*) promoter (Merritt et al., 2005) and cloned into pFW5 vector to generate pFW5Φ(*ldh*$_p$-leading sequence-*gfp-spaP*). The recombinant construct was transformed into *S. mutans* strain UA140 as well as the *prsA*-deficient mutant to generate the cell surface displayed GFP-SpaP fusion derivative (Guo *et al.*, unpublished data), respectively. The integration of *gfp-spaP* into the chromosome of *S. mutans* via single crossover homologous recombination was confirmed by PCR, and cell surface localization of the GFP-SpaP fusion was revealed by Western blot analysis using an anti-GFP antibody (Guo *et al.*, unpublished data).

General phenotypic characterization assays

Growth kinetics were measured for *S. mutans* UA140, the *prsA*-deficient strain and the strain containing the cell surface displayed GFP. Autolysis assay was also performed as previously described (Wen & Burne, 2002).

Hydrophobicity assay by the bacterial adherence to hydrocarbons (BATH)

The bacterial hydrophobicity was measured using the BATH method as described previously (Dillon *et al.*, 1986). Briefly, the bacterial cultures which were dispersed by drawing up and expelling the bacterial suspension 10 times through a 26 gauge, 5/8 inches (15.9 mm) long needle (Dunning *et al.*, 2008) were suspended in PUM buffer (K_2HPO_4, 16.87 g/L; KH_2PO_4, 7.26 g/L; $MgSO_4{\cdot}7H_2O$, 0.2 g/L; urea, 1.8 g/L; pH 7.1) to a final OD_{600} of 0.6. A 1.2 mL volume of the bacterial suspension was dispensed into each one of 12 round bottom test tubes with 10 mm in diameter. Four tubes with four different volumes (0.2, 0.15, 0.1, and 0.05 mL) of N-hexadecane were kept at room temperature for 10 min, vortex-mixed for 2 min and followed by incubation at room temperature for 15 min to allow hydrocarbon separation. The absorbance at 400 nm of the aqueous phase was measured before and after treatment (Spectronic Genesys 5 UV-Visible Spectrophotometers) and results were recorded as the percentage absorbance of the aqueous phase after treatment relative to the initial absorbance of the bacterial suspension.

Atomic force microscopy (AFM) force spectroscopy

AFM force spectroscopy was performed to measure cell hydrophobicity. AFM force-distance curves were obtained in deionized water using a combined inverted optical (Bruker, Santa Barbara, CA) system. Oxide-sharpened microfabricated Si_3N_4 cantilevers with a spring constant of 0.01 N/m (MLCT, Bruker, Santa Barbara, CA) were coated by electron beam thermal evaporation with a 5-nm-thick Cr layer followed by a 30-nm-thick Au layer (Sharma *et al.*, 2009). Gold-coated cantilevers were immersed for 14 h in 1 mM solutions of HS $(CH_2)_{11}CH_3$ in ethanol and then rinsed with ethanol. To probe *S. mutans* cell surface hydrophobicity, cells were grown on glass cover-slips for 3 h in TH medium supplemented with 0.5% sucrose. Surface immobilization of the bacterial cells was tested by gently imaging them at low forces (~200pN) prior to force curve measurements. Force-distance curves over a 400 × 400 nm area were obtained using hydrophobic tips with z ramp size of 10μms, 1024 × 1024 samples/line and 0.5Hz. The adhesion strength was calculated for each force curve using SPIP™ software (Image Metrology, Horsholm, Denmark.).

Sonication-resistance analysis

The resistance of *S. mutans* UA140 and its *prsA*-deficient derivative to sonication was assayed by monitoring the bacterial viability after sonication treatment. Bacterial suspensions with a density of 10^9 CFU/ml were prepared from overnight cultures and subjected to sonication at a constant frequency of 22 kHz and output power of 10 watts for different periods of time ranging from 1 to 9 min. Cell viability after sonication treatment was determined by CFU counting on TH agar plates.

Early biofilm formation assay

In order to compare the sucrose-independent and sucrose-dependent adhesion abilities between *S. mutans* UA140 wild-type and the *prsA*-deficient mutant, overnight cultures of both strains were dispersed by needle and syringe, and resuspended in glucose or sucrose-supplemented (20 mM) minimal medium (Loo *et al.*, 2000) to a final OD_{600} of 0.1. Four hundred μL of bacterial suspension was added to the well of a 24-well flat-bottomed polystyrene microtiter plate (Corning, New York, NY). After 3 h incubation in the presence of 5% CO_2, the plates were rinsed with PBS for three times to remove planktonic and loosely bound cells. The biofilms were detached using cell scrapers (Thermo, Rochester, NY) and clumps were broken up and dispersed by needle and syringe. The biomass of early biofilm was then calculated as CFU/mL by viability counting on agar plates.

Scanning electron microscopy (SEM)

Overnight cultures of *S. mutans* UA140 and its *prsA*-deficient derivative were harvested and resuspended in fresh TH medium to an OD_{600} of 0.6. A 100-fold dilution of the bacterial suspension into defined minimal medium supplemented with 0.5% (wt/vol) sucrose was then added to each well of six-well polystyrene microtiter plates in which sterile coverglasses had been placed. After 16 h incubation, the medium containing the remaining planktonic cells was aspirated and the cover glasses were carefully rinsed twice with 1 mL PBS without disturbing the attached biofilms. The biofilms were fixed with 1% glutaraldehyde. After another wash with phosphate buffer, the samples were mounted on a stub with silver adhesive (Electron Microscopy Sciences, Hatfield, PA, U.S.A.), sputter coated with a 40-nm layer of platinum and examined with an SEM operating at 5 kV in the secondary electron mode (XL 30 S, FEG, FEI Company, Hillsboro, OR, U.S.A.).

SDS-PAGE

Cell wall/membrane was prepared from *S. mutans* as described by Yamashita *et al.* (1998) with some modifications. Briefly, bacterial cells from the overnight cultures were collected

by centrifugation. The cell pellets were resuspended in 50mM Tris·HCl (pH 8.0) containing 1 mM PMSF, transferred to a chilled 2 ml microcentrifuge tube containing 425–600μm diameter glass beads (Sigma) and disrupted with a Mini-Bead Beater homogenizer (Biospec Products) for 10 min. The glass beads were removed and undisrupted cells were separated by centrifugation at 2,000 × g for 10 min. The supernatants were further centrifuged at 150,000 × g for 2 h to collect the crude cell wall fraction. The pellets were washed twice with warm distilled water and resuspended in 50mM Tris•HCl (pH 8.0) containing 1 mM EDTA, 1 mM PMSF, 10 mg/L RNase and 10 mg/L DNase and incubated at 37°C for 1 h. The samples were boiled in SDS-PAGE loading buffer for 10 min before being loaded onto 10% SDS-PAGE gel. The protein concentration was determined by the Bradford method with the Pierce BCA protein assay kit (Thermo, Rockford, IL, USA).

Glucan Analysis

Overnight cultures of *S. mutans* strains were collected by centrifugation at 6,000 × g for 5 min. The pellets were washed twice with PBS and resuspended in minimal defined medium to a cell density of 10^8 cells/ml. Sucrose was added to the cell suspension to a final concentration of 100 mM. The cells were incubated at 37°C for 16 h in the presence of 5% CO_2, and collected by centrifugation at 10,000 × g for 10 min. Pellet and supernatant were used to assess the production of insoluble and soluble glucan, respectively. For soluble glucan analysis, the supernatant was precipitated by chilled ethanol. As for insoluble glucan analysis, the pellet was washed with distilled water three times to remove the remaining soluble glucan. NaOH (1.0 N) was added and the alkali-soluble polysaccharides were precipitated with chilled ethanol. The amounts of glucan were measured by the phenol sulphuric acid method (Dubois *et al.*, 1956). A derivative of *S. mutans* UA140 lacking *gtfBC* (kindly provided by H. Kuramitsu, University of Buffalo, NY, USA) was used as a negative control.

Mutacin IV production assay

Mutacin IV production was measured by deferred antagonism according to the protocol by Tsang *et al.* (2006). Five microlitres of *S. mutans* overnight culture was spotted onto TH agar plates and the plates were incubated at 37°C in the presence of 5% CO_2. After 16 h incubation, 5 mL of a soft agar overlay containing *S. sanguinis* ATCC 10556 or *S. gordonii* DL1 at an OD_{600} of 0.1 as indicator strain was poured on top of the plates spotted with *S. mutans*. The growth inhibition zone of *S. sanguinis* or *S. gordonii* in the overlay agar was inspected after overnight incubation. The distance from the colony edge to the edge of the clearance zone was measured to calculate the inhibition area. Results are expressed as percentage of inhibition area induced by the *prsA* mutant relative to its parent strain.

Confocal laser scanning microscope (CLSM)

The 3-h biofilms of *S. mutans* GFP-SpaP fusion derivatives of wild type and the *prsA* mutant were formed according to aforementioned procedure in the section of early biofilm formation assay except a final OD600 of 0.3 was used for the mutant in order to normalize the number of bacteria attached to the well. Biofilms were grown in medium supplemented with sucrose in each well of a sterile 8-well Lab-Tek™ Chambered Coverglass (Nalge Nunc International; Naperville, IL). The biomass of wild type and *prsA* mutant strains was normalized according to their respective CFU counts. All biofilm images were collected with a Zeiss LSM 5 PASCAL confocal laser scanning microscope (CLSM) using LSM 5 PASCAL software (Zeiss, Jena, Germany). Excitation at 488 nm with an argon laser in combination with a 505–530 nm bandpass emission filter was used for GFP fluorescence imaging. The scanning module of the system was mounted onto an inverted microscope (Axiovert 200M). A 40 oil-immersion objective (numerical aperture 1.3) was used for imaging. Image stacks (1024 by 1024-pixel tagged image file format) of eight randomly

chosen spots were collected for each biofilm and quantified using the image analysis software COMSTAT. The fluorescence intensities in the biofilms of *S. mutans* GFP-SpaP strain and its *prsA*-deficient derivative were normalized to the number (CFU counts) of bacteria present in the well.

RESULTS

Bioinformatic analysis revealed the presence of a *prsA* gene in the *S. mutans* genome. Sequence homology analysis showed that the *prsA* gene of *S. mutans* exhibited 69% homology to the one found in *Streptococcus agalactiae*, 67% homology to *Streptococcus pyogenes*, and 66% homology to *Streptococcus dysgalactiae* at the nucleotide level. The deduced PrsA amino acid sequences exhibited a homology of ~57–62% to other PrsA proteins among these streptococci, suggesting that PrsA from these streptococci are not well conserved. And the PrsA from *S. mutans* displayed only 32% identity to the PrsA of *Bacillus subtilis*. Since there are two types of PrsA proteins differing in the presence or absence of peptidyl-prolyl *cis/trans*-isomerases (PPIase) signature motif, the PrsA protein sequence of *S. mutans* was further aligned with both the *B. subtilis* and *Listeria monocytogenes* PrsA sequence using the ClustalW tool (www.ebi.ac.uk/clustalw). However, the signature motif for PPIase is absent in *S. mutans* PrsA.

prsA deletion mutant auto-aggregates when grown as planktonic culture

The expression of the downstream gene of *prsA* is not affected by the *prsA* deletion mutant construction method (data not shown). The disruption of *prsA* did not affect cell viability either, and no significant difference in cell autolysis was observed between the *prsA* mutant and its parent strain (data not shown). However, the *prsA*-deficient strain displayed a striking auto-aggregation phenotype and the cells tended to clump and precipitate at the bottom of the glass tubes, while the wild-type strain showed a uniformly turbid appearance in TH medium after overnight growth (Fig 1A). Light microscopy observations showed that the mutant strain formed about 12 clumps per field of view, in contrast to the parent strain for which no clumps were observed (Fig 1B and C).

prsA-deficient strain has altered cell surface characteristics

Enhanced auto-aggregation could result from altered cell surface properties, thus we examined the cell surface hydrophobicity of the *prsA* mutant. Using the BATH assay, we demonstrated that the percentage absorbance of the aqueous phase in the *prsA* mutant after treatment with hydrocarbon relative to the initial absorbance was significantly less than that of the parent strain (37% vs. 61%) (Fig 2A), suggesting an increased bacterial surface hydrophobicity in *prsA*-deficient strain. Cell surface hydrophobicity was also quantitatively measured using chemically modified AFM. Fig. 2B shows the adhesion histograms and representative force curves obtained for the *prsA*-deficient and wild type strains. “Saw tooth-like” force rupture events were observed in the retract regions of the force curves with hydrophobic tips (shown in inset images in 2B). Adhesion forces measurements showed higher adhesion forces over *prsA*-deficient cell surfaces compared to wild-type cell surfaces with mean values of 370±17pN and 120±12pN respectively. These results confirm the qualitative findings obtained from the BATH assay at the single bacterial level and indicate that the *prsA*-deficient strain is about three-fold more hydrophobic compared to the wild-type ($P<0.05$).

Sonication was used as a measure of the degree of physical cell membrane integrity. Results showed that, after 5 min sonication treatment, the *prsA* mutant suffered a drastic reduction (about 300-fold) in viability compared to the wild type (~3-fold) (Fig 2C), indicating that deletion of the *prsA* gene renders cells more sensitive to sonication-induced lysis.

The *prsA*-deficient strain displays reduced early biofilm formation and forms overnight biofilms with aberrant architecture

Our data revealed that lack of *prsA* resulted in altered cell surface characteristics. Since surface properties are important for cell adherence and biofilm formation, we further investigated the effect of PrsA on these phenotypes. Bacterial counts showed an almost 100-fold reduction in the number of attached *prsA*-deficient cells compared to the wild-type (Fig 3A). Interestingly, when sucrose was replaced by glucose, both strains formed similar thin biofilms and the bottom of the well was not evenly covered with cells.

SEM analysis of biofilms grown on the surfaces of glass in defined medium with sucrose revealed that wild-type biofilms presented a uniform, sieve-like appearance with thick and compact layers of cells. In contrast, the mutant strain formed more compact microcolonies compared to its parent strain.

The *prsA*-deficient strain shows reduced insoluble glucan and mutacin IV production as well as the heterologous protein GFP-SpaP

Since PrsA has been shown to be involved in the post-export of a variety of exoproteins in *Bacillus* (Jacobs et al., 1993; Vitikainen et al., 2001), we suspected that the deletion of *prsA* might affect the profile of cell wall/ membrane proteins in *S. mutans* as well. As shown in Fig 4A, the *prsA*-deficient strain displayed an altered cell wall/ membrane protein profile compared to the wild type, with some protein bands showing increased intensity, while others exhibiting an obvious reduction. Since the effect of PrsA on cell wall/ membrane proteins is relatively general, we chose several known exoproteins for further characterization.

SEM imaging analysis revealed that the *prsA* mutant biofilm had less extracellular matrix compared to that of the wild type (Fig 3B). In *S. mutans*, cell wall associated glucosyltransferases (GTF) are responsible for synthesizing glucan, one of the main components of the extracellular matrix. Since deletion of *prsA* could potentially affect translocation of GTF proteins to the cell surface and thus alter glucan production, we determined the glucan production ability in both strains. Our results showed that the *prsA*-deficient strain produced less insoluble glucan compared to the wild-type (Fig 4B), while no difference in soluble glucan production was observed.

Furthermore, the effect of the *prsA* deletion on mutacin IV, a well-known secreted peptide bacteriocin was investigated. The deferred antagonism assay showed that the inhibition zone produced by the *prsA*-deficient strain was 49.67±4.20% and 50.39±4.52% of the one produced by the wild type using *S. gordonii* DL1 and *S. sanguinis* ATCC 10556 as indicator strains (Fig 4C).

To investigate whether PrsA facilitates the folding of exported heterologous proteins, we constructed derivatives of *S. mutans* wild type and *prsA* mutant, both displaying a GFP protein on the cell surface via a fusion to SpaP. Our previous study showed that fusion of GFP to SpaP resulted in surface localization and efficient folding of GFP with proper function (unpublished). Therefore, the post-export folding of heterologous protein GFP can be analyzed based on the fluorescence intensity of fused GFP. By quantifying image stacks of three randomly chosen biofilm spots, we found that the fluorescence intensity and thus the GFP surface display was reduced in the *prsA* mutant biofilm (> 3-fold) compared to the wild-type (Fig 4D).

DISCUSSION

S. mutans secretes numerous proteins (enzymes)/peptides that play crucial roles in competing with other bacteria and establishing itself within oral cavity via biofilm formation. The expression and activity of these exoproteins have been shown to be regulated at multiple levels, including post-translational as well as translocation regulation. In this study, we report the identification of PrsA, a predicted foldase that is involved in the post-export of a variety of proteins including membrane-associated proteins in *S. mutans.*

The auto-aggregation phenotype, as well as increased cell surface hydrophobicity and reduced resistance to mechanical breakage indicated a substantial change in the cell surface structure and properties upon deletion of the *prsA* gene. This was further corroborated by our AFM data showing the “saw tooth-like” force rupture patterns between hydrophobic AFM probes and *prsA*-deficient strains (Fig. 2B), which often reflects the unfolding of cell surface-bound proteins (Rief *et al.*, 1998; Hu *et al.*, 2011). As demonstrated in other Gram-positive bacteria such as *Bacillus* and *Lactococcus,* PrsA acts as a chaperone to assist the folding and stability of exported proteins (Lindhom *et al.*, 2006; Wahlström *et al.*, 2003). Thus, the presence of unfolded proteins on the cell surface of the PrsA-deficient *S. mutans* derivative would be consistent with a role of PrsA as a cell surface chaperone in *S. mutans* similar to findings in other species. The notion that the PrsA of *S. mutans* has roles similar to the ones extensively researched especially in *B. subtilis* is further sustained by the observed differences in the cell wall/ membrane protein profile of the *prsA* mutant compared with its parent strain (Fig. 4A). In a recent proteome analysis, PrsA-depleted *B. subtilis* cells were found to differentially secrete almost 200 proteins (Hyyryläinen *et al.*, 2010).

Further phenotypic analysis of the PrsA deficient *S. mutans* derivative indicated that one group of proteins affected by PrsA function are the glycosyl transferases of *S. mutans*. The *prsA*-deficient strain exhibited a significant decrease in insoluble glucan production which resulted in reduced sucrose-dependent adhesion and biofilm formation (Fig. 3). It is well known that the majority of dental biofilm matrix is rich in polysaccharides (Paes Leme *et al.*, 2006), of which glucan is one of the main components. These glucan-rich matrix could provide binding sites that promote accumulation of microorganisms on the tooth surface and further establishment of pathogenic biofilms (Koo *et al.*, 2010). *S. mutans* encodes three GTFs. GtfB synthesizes mostly insoluble glucan, GtfC forms a mixture of insoluble and soluble glucan, while GtfD produces predominantly soluble glucan (Paes Leme *et al.*, 2006). The insoluble glucan contributes to the glue-like characteristics of dental biofilms (Xiao et al., 2012). *S. mutans* strains deficient in insoluble glucan production are essentially non-cariogenic in a rodent model (Yamashita *et al.*, 1993). While deletion of *prsA* resulted in a near 60% reduction in insoluble glucan production, it did not affect soluble glucan production, suggesting that PrsA might be involved in the post-export and/ or function of GTF B and C, but not GTF D.

Mutacin is a known secreted bacteriocin and has been implicated as virulence factor of *S. mutans* (Kuramitsu, 1993). *S. mutans* strain UA140 could produce both mutacin I and IV (Qi *et al.*, 2001). Our results indicated reduced mutacin IV in the *prsA* mutant. This correlates well with previous related studies in other Gram-positive bacteria, where PrsA has been shown to be involved in the post-export of a variety of virulence factors. However there was no difference in mutacin I between the wild type and the *prsA* mutant (data not shown). In *Bacillus* species, α-amylase, β-glucannase and lipoproteinβ-lactamase were exported in a PrsA dependent manner (Jacobs *et al.*, 1993; Vitikaninen *et al.*, 2005), while over-expression of PrsA has been shown to increase the secretion of major bacillary exoenzymes (Kontinen & Sarvas, 1993). In Group A streptococcus, genomic disruption of

prsA decreased the production of enzymatically active streptococcal pyrogenic exotoxin (SpeB) but not the level of the pro-SpeB zymogen (Ma *et al.*, 2006).

The function of heterologous protein is mainly limited by the post-translational events including the inefficient translocation and folding of proteins and protease degradation (Tjalsma *et al.*, 2004) and PrsA has been suggested to facilitate the folding of exported proteins into their final, mature conformation (Jacobs *et al.*, 1993). In this study, we found that the fluorescence signal of a surface displayed GFP-SpaP fusion protein was reduced in the *S. mutans* strain lacking *prsA*. This result is consistent with observations that there was a positive correlation between the level of PrsA and the amount of a surface-localized fusion protein consisting of *S. mutans* SpaP and the pertussis toxin S1 fragment following expression in the heterologous host *S. gordonii* (Davis *et al.*, 2011). Furthermore, the level of PrsA was found linearly proportional to protein secretion rate in *B. subtilis* (Vitikainen *et al.*, 2001); while overproduction of PrsA could increase stability of the amylase and the protective antigen from *B. subtilis* (Kontinen & Sarvas, 1993; Vitikaninen *et al.*, 2005; Williams *et al.*, 2003), and prevent degradation of proteins on the cell surface of *L. lactis* (Drouault *et al.*, 2002).

GTFs contain amino-terminal signal peptide which is thought to direct these proteins to the Sec secretory pathway (Navarre & Schneewind, 1999); while mutacin might be translocated by a specific ATP-binding transporter (van Belkum *et al.*, 1997). The involvement of PrsA in GTF and mutacin IV production as demonstrated in this study suggested that, like foldase homologues identified in many other gram positive bacteria, PrsA may work closely with cellular export machineries in assisting the folding of a variety of exoproteins in *S. mutans*.

Acknowledgments

We thank H. Kuramitsu from the University of Buffalo (NY, USA) for kindly providing the *gtfBC*-deficient derivative of *S. mutans* UA140. This work was supported by a grant from the National Institute of Health (NIH-1-R01-DE020102) and a grant from the Natural Sciences Foundation of China (30672322). Dr. Wenyuan Shi wishes to disclose his potential Conflict of Interests here as he serves as a part time chief science officer of C3 Jian Inc, a California-based biotechnology company which is developing technologies to eliminate *S. mutans* within human oral cavities.

References

Ahimou F, Denis FA, Touhami A, Dufrene YF. Probing microbial cell surface charges by atomic force microscopy. Langmuir. 2002; 18:9937–9941.

Alsteens D, Dague E, Rouxhet PG, Baulard AR, Dufrêne YF. Direct measurement of hydrophobic forces on cell surfaces using AFM. Langmuir. 2007; 23:11977–11979. [PubMed: 17941657]

Davis E, Kennedy D, Halperin SA, Lee SF. Role of the cell wall microenvironment in expression of a heterologous SpaP-S1 fusion protein by *Streptococcus gordonii*. Appl Environ Microbiol. 2011; 77:1660–1666. [PubMed: 21193663]

Dillon JK, Fuerst JA, Hayward AC, Davis GHG. A comparison of five methods for assaying bacterial hydrophobicity. J Microbiol Method. 1986; 6:13–19.

Drouault S, Anba J, Bonneau S, Bolotin A, Ehrlich SD, Renault P. The peptidyl-prolyl isomerase motif is lacking in PmpA, the PrsA-like protein involved in the secretion machinery of *Lactococcus lactis*. Appl Environ Microbiol. 2002; 68:3932–3942. [PubMed: 12147493]

Dubois M, Gilles KA, Hamilton JK, Rebers PA, Smith F. Colorimetric method for determination of sugars and related substance. Anal Chem. 1956; 28:350–356.

Dunning DW, McCall LW, Powell WF, et al. SloR modulation of the *Streptococcus mutans* acid tolerance response involves the GcrR response regulator as an essential intermediary. Microbiol. 2008; 154:1132–1143.

Fekkes P, Driessen AJ. Protein targeting to the bacterial cytoplasmic membrane. Microbiol Mol Biol Rev. 1999; 63:161–173. [PubMed: 10066835]

Hale JDF, Ting YT, Jack RW, Tagg JR, Heng NCK. Bacteriocin (mutacin) production by *Streptococcus mutans* genome sequence reference strain UA 159: Elucidation of the antimicrobial repertoire by genetic dissection. Appl Environ Microbiol. 2005; 71:7613–7617. [PubMed: 16269816]

Hamada S, Slade HD. Biology, immunology, and cariogenicity of *Streptococcus mutans*. Microbiol Rev. 1980; 44:331–384. [PubMed: 6446023]

Hu Y, Ulstrup J, Zhang J, Molin S, Dupres V. Adhesive properties of *Staphylococcus epidermidis* probed by atomic force microscopy. Physical chemistry chemical physics : PCCP. 2011; 13:9995–10003. [PubMed: 21350761]

Hyyryläinen HL, Bolhuis A, Darmon E, et al. A novel two-component regulatory system in *Bacillus subtilis* for the survival of severe secretion stress. Mol Microbiol. 2001; 41:1159–1172. [PubMed: 11555295]

Hyyryläinen HL, Marciniak BC, Dahncke K, et al. Penicillin-binding protein folding is dependent on the PrsA peptidyl-prolyl *cis-trans* isomerase in *Bacillus subtilis*. Mol Microbiol. 2010; 77:108–127. [PubMed: 20487272]

Jacobs M, Andersen JB, Kontinen V, Sarvas M. *Bacillus subtilis* PrsA is required *in vivo* as an extracytoplasmic chaperone for secretion of active enzyme synthesized either with or without pro-sequences. Mol Microbiol. 1993; 8:957–966. [PubMed: 8102773]

Kelly C, Evans P, Bergmeier L, et al. Sequence analysis of the cloned streptococcal cell surface antigen I/II. FEBS Lett. 1989; 258:127–132. [PubMed: 2687020]

Kontinen VP, Sarvas M. The PrsA lipoprotein is essential for protein secretion in *Bacillus subtilis* and sets a limit for high-level secretion. Mol Microbiol. 1993; 8:727–737. [PubMed: 8332065]

Koo H, Xiao J, Klein MI, Jeon JG. Exopolysaccharides produced by *Streptococcus mutans* glucosyltransferases modulate the establishment of microcolonies within multispecies biofilms. J Bacteriol. 2010; 192:3024–3032. [PubMed: 20233920]

Kreth J, Merritt J, Shi W, Qi F. Coordinated bacteriocin production and competence development: a possible mechanism for taking up DNA from neighbouring species. Mol Microbiol. 2005; 57:392–404. [PubMed: 15978073]

Kuramitsu HK. Virulence factors of mutans streptococci: role of molecular gentics. Crit Rev Oral Biol Med. 1993; 4:159–176. [PubMed: 8435464]

Lindholm A, Ellmen U, Tolonen-Martikainen M, Palva A. Heterologous protein secretion in *Lactococcus lactis* is enhanced by the Bacillus subtilis chaperone-like protein PrsA. Appl Microbiol Biotechnol. 2006; 73:904–914. [PubMed: 16944130]

Loo CY, Corliss DA, Ganeshkumar N. *Streptococcus gordonii* biofilm formation: identification of genes that code for biofilm phenotypes. J Bacteriol. 2000; 182:1374–1382. [PubMed: 10671461]

Ma Y, Bryant AE, Salmi DB, et al. Identification and characterization of bicistronic *speB* and *prsA* gene expression in the group A *Streptococcus*. J Bacteriol. 2006; 188:7626–7634. [PubMed: 16950917]

Matias VR, Beveridge TJ. Native cell wall organization shown by cryo-electron microscopy confirms the existence of a periplasmic space in *Staphylococcus aureus*. J Bacteriol. 2006; 188:1011–1021. [PubMed: 16428405]

Matias VR, Beveridge TJ. Lipoteichoic acid is a major component of the *Bacillus subtilis* periplasm. J Bcteriol. 2008; 190:7414–7418.

Merritt J, Kreth J, Shi W, Qi F. LuxS controls bacteriocin production in *Streptococcus mutans* through a novel regulatory component. Molecular Microbiol. 2005; 57:960–969.

Muller M, Koch HG, Beck K, Schafer U. Protein traffic in bacteria: multiple routes from the ribosome to and across the membrane. Prog Nucl Acid Res Mol Biol. 2001; 66:107–157.

Navarre WW, Schneewind O. Surface proteins of Gram-positive bacteria and mechanisms of their targeting to the cell wall envelope. Microbiol Mol Biol Rev. 1999; 63:174–229. [PubMed: 10066836]

Paes Leme AF, Koo H, Bellato CM, Bedi G, Cury JA. The role of sucrose in cariogenic dental biofilm formation-new insight. J Dent Res. 2006; 85:878–887. [PubMed: 16998125]

Podbielski A, Spellerberg B, Woischnik M, Pohl B, Lutticken R. Novel series of plasmid vectors for gene inactivation and expression analysis in group A streptococci (GAS). Gene. 1996; 177:137–147. [PubMed: 8921859]

Qi F, Chen P, Caufield PW. The group I strain of *Streptococcus mutans*, UA140, produces both the lantibiotic mutacin I and a nonlantibiotic bacteriocin, mutacin IV. Appl Environ Microbiol. 2001; 67:15–21. [PubMed: 11133423]

Rief M, Gautel M, Schemmel A, Gaub HE. The mechanical stability of immunoglobulin and fibronectin III domains in the muscle protein titin measured by atomic force microscopy. Biophys J. 1998; 75:3008–30014. [PubMed: 9826620]

Sarvas M, Harwood CR, Bron S, van Dijl JM. Post-translocational folding of secretory proteins in Gram-positive bacteria. Biochim Biophys Acta. 2004; 1694:311–327. [PubMed: 15546674]

Sharma S, Cross SE, French S, et al. Influence of substrates on Hepatocytes: a nanomechanical study. J Scanning Probe Microscopy. 2009; 4:7–16.

Tjalsma H, Antelmann H, Jongbloed JD, et al. Proteomics of protein secretion by *Bacillus subtilis*: separating the “secrets” of the secretome. Microbiol Mol Biol Rev. 2004; 68:207–233. [PubMed: 15187182]

van Belkum MJ, Worobo RW, Stiles ME. Double-glycine-type leader peptides direct secretion of bacteriocins by ABC transporters: colicin V secretion in *Lactococcus lactis*. Mol Microbiol. 1997; 23:1293–1301. [PubMed: 9106219]

Vitikainen M, Pummi T, Airaksinen U, et al. Quantitation of the capacity of the secretion apparatus and requirement for PrsA in growth and secretion of alpha-amylase in *Bacillus subtilis*. J Bacteriol. 2001; 183:1881–1890. [PubMed: 11222585]

Vitikaninen M, Hyyryläinen HL, Kivimäki A, Kontinen VP, Sarvas M. Secretion of heterologous proteins in *Bacillus subtilis* can be improved by engineering cell components affecting post-translocational protein folding and degradation. J Appl Microbiol. 2005; 99:363–375. [PubMed: 16033468]

Wahlström E, Vitikainen M, Kontinen VP, Sarvas M. The extracytoplasmic folding factor PrsA was thought to be required for protein secretion only in the presence of the cell wall, in *Bacillus subtilis*. Microbiol. 2003; 149:569–577.

Wen ZT, Burne RA. Functional genomics approach to identifying genes required for biofilm development by *Streptococcus mutans*. Appl Environ Microbiol. 2002; 68:1196–1203. [PubMed: 11872468]

Williams RC, Rees ML, Jacobs MF, et al. Production of *Bacillus anthracis* protective antigen is dependent on the extracellular chaperone, PrsA. J Biol Chem. 2003; 278:18056–18062. [PubMed: 12606539]

Xiao J, Klein MI, Falsetta ML, et al. The exopolysaccharide matrix modulates the interaction between 3D architecture and virulence of a mixed-species oral biofilm. PLoS Pathog. 2012; 8:e1002623. [PubMed: 22496649]

Yamashita Y, Bowen WH, Burne RA, Kuramitsu HK. Role of the *Streptococcus mutans gtf* genes in caries induction in the specific-pathogen-free rat model. Infect Immun. 1993; 61:3811–3817. [PubMed: 8359902]

Yamashita Y, Tsukioka Y, Nakano Y, Tomihisa K, Oho T, Koga T. Biological functions of UDP-glucose synthesis in *Streptococcus mutans*. Microbiol. 1998; 144:1235–1245.

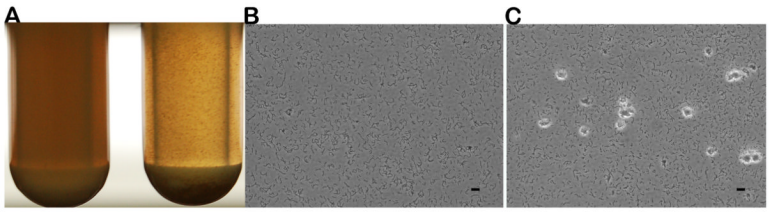

Figure 1.
Cell morphological characteristics in TH medium. 24-h cultures of *S. mutans* UA140 (left) and the *prsA*-deficient strain (right) (A). Light microscopic observation of a 24-h culture of *S. mutans* UA140 (magnification, ×400) (B) and the *prsA*-deficient strain (C). The scale bar equals to 10 μm.

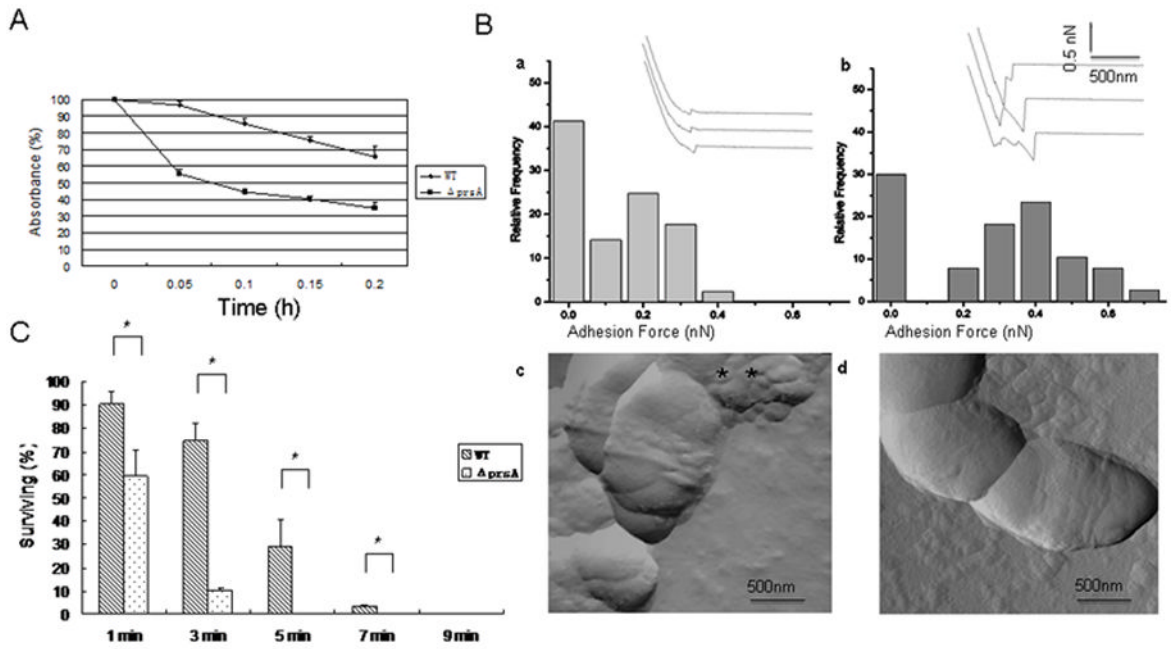

Figure 2.

Cell surface characteristics. (A) Hydrophobicity: Adherence of *S. mutans* UA140 wild type and its *prsA*-deficient derivative to hexadecane in the BATH assay. Results are expressed as percentage absorbance of the aqueous phase after hexadecane treatment relative to the initial absorbance. Each point represents the mean of three independent experiments. (B) AFM analysis: Adhesion histograms and representative force curves (inset) recorded with hydrophobically modified tips on *S. mutans* UA140 (a) and the *prsA*-deficient strain (b) using a maximum applied force of 1nN. The surface topographies of wild type (c) and mutant strain (d) were also observed (amplitude images) using high-resolution AFM imaging. Two biological replicates were performed and representative image are shown. (C) Resistance of *S. mutans* UA140 and the *prsA*-deficient strain to sonication at a constant frequency of 22 kHz. Results are expressed as percentage of viable cells after sonication relative to untreated cells. Each point represents the mean ± SD of two independent measurements. The asterisk indicates that *prsA*-deficient strains were significantly less resistant to sonication than wild type at the same treatment time point (Student's t test p value <0.05).

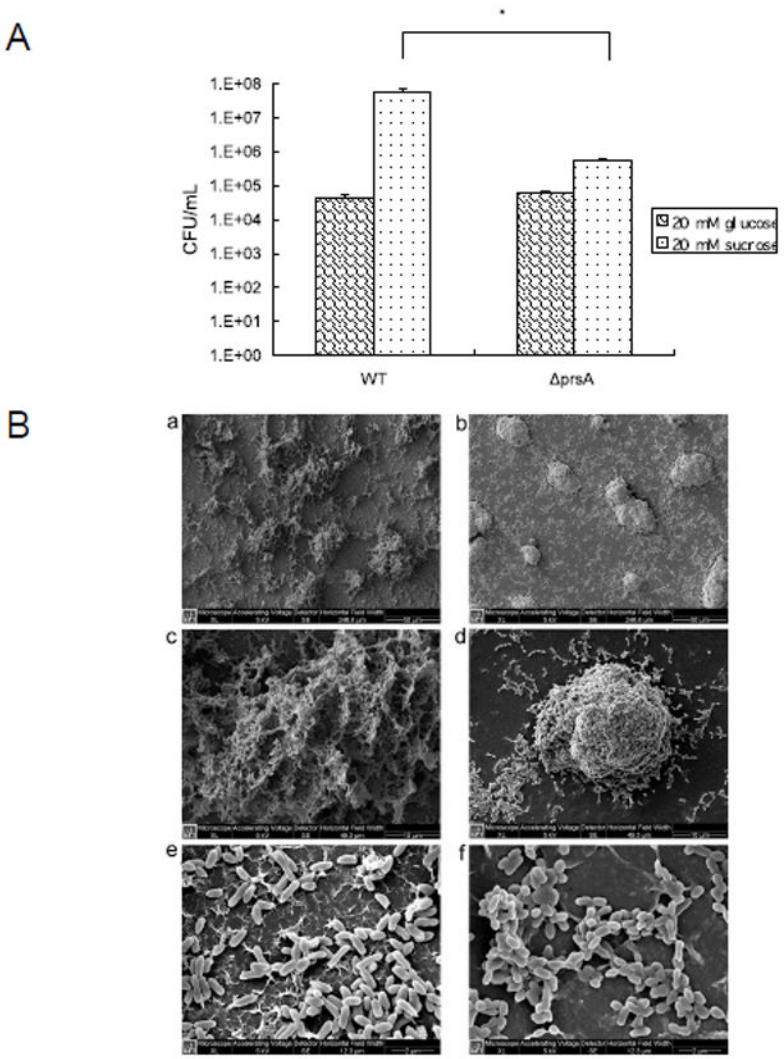

Figure 3.

Biofilm formation characteristics. (A) Early Biofilm formation of *S. mutans* UA140 wild type and the *prsA*-deficient strains in minimal defined medium supplemented with glucose or sucrose. Each data point is the average of triplicate samples, and the error bars correspond to the standard deviations. The asterisk indicates that there was significantly less *prsA* mutant cells attached to the well of a 24-well flat-bottomed polystyrene microtiter plate than wild type in the presence of sucrose (Student's t test p value <0.05). (B) Scanning electron micrographs of *S. mutans* 16 h-biofilms formed on glass surfaces. *S. mutans* UA140 wild-type biofilms (a, c, e); *prsA*-deficient strain biofilms (b, d, f). Magnifications, ×1000 (a, b), ×5000 (c, d) and ×20000 (e, f).

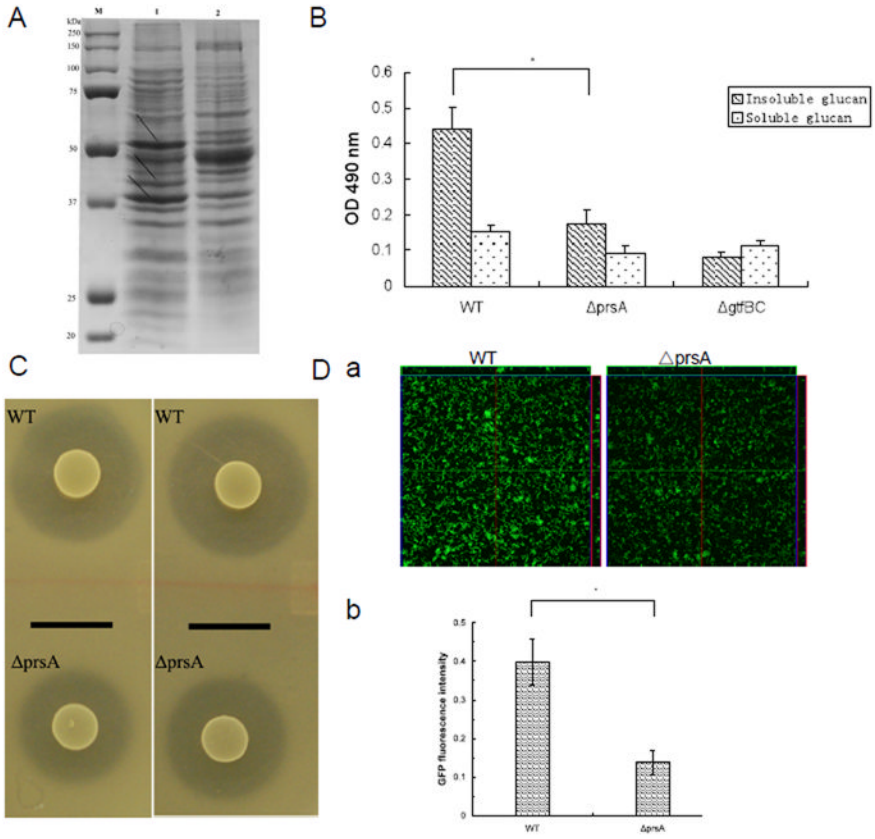

Figure 4.

Analysis of PrsA-dependent phenotypes. (A) SDS-PAGE (10%) analysis of cell cell wall/ membrane proteins from *S. mutans* UA140 and the *prsA*-deficient strain. Lanes: M, prestained protein markers (Bio-rad); 1, *S. mutans* UA140; 2, UA140 *prsA*-deficient strain. Arrows indicate differentially expressed cell wall/ membrane proteins. (B) Glucan production of *S. mutans* UA140 wild type and the *prsA*-deficient strains in TH medium supplemented with 100 mM sucrose. *S. mutans* UA140 *gtfBC*-deficient strain was used as a negative control. Each data point is the average of triplicate samples, and the error bars indicate standard deviations. The asterisk indicates that *prsA*-deficient strain produced significantly less insoluble glucan than wild type (Student's t test p value <0.05). (C) Drop inoculum deferred antagonism assay for *S. mutans* UA140 wild type and the *prsA*-deficient strains. The clear zone indicates mutacin IV production. The indicator strains are *S. sanguinis* (left panel) and *S. gordonii* (right panel) respectively. (D) GFP fluorescent signals of 3-h biofilms of *S. mutans* wild-type and the *prsA*-deficient, both carrying surface-displayed GFP-SpaP fusion protein. (a) CLSM analysis of surface-expressed GFP fluorescent signals within biofilms. (b) Quantification of GFP fluorescent signals within biofilms. The fluorescence intensities of *S. mutans* wild-type and the *prsA*-deficient biofilms were normalized to the number (CFU counts) of bacteria present in the well. The GFP expression percentage was calculated as the amount of fluorescence signal of *prsA*-deficient strain of *vs* its parent strain.